Supporting Information

Viscoelasticity of polyethylene glycol solutions on supported lipid bilayer by quartz crystal microbalance with dissipation

Ziliang Zhao,[†,§] *Xiangling Ji,*[*,†] *Rumiana Dimova,*[‡] *Reinhard Lipowsky,*[‡] *Yonggang Liu*[*,†,‡]

[†] State Key Laboratory of Polymer Physics and Chemistry, Changchun Institute of Applied Chemistry, Chinese Academy of Sciences, 130022 Changchun, China

[‡] Department of Theory and Bio-Systems, Max Planck Institute of Colloids and Interfaces, Science Park Golm, 14424 Potsdam, Germany

[§] University of Chinese Academy of Sciences, 100049 Beijing, China

[*] Corresponding author: xlji@ciac.ac.cn (X.J.); yonggang@ciac.ac.cn (Y.L.)

Molecular weight distribution of PEG and PEO samples. The molecular weights of 12 PEG samples and 3 PEO samples were determined by a gel permeation chromatography equipped with either two PL aquagel-OH 30 or two PL aquagel-OH mixed-H columns (7.5×300mm) with refractive index detection. Water containing 0.02% NaN_3 was used as the eluent at a flow rate of 1.0 mL/min. The columns were calibrated with narrow PEG/PEO standards from Polymer Laboratories Ltd. Table S1 summarized the molecular weight data of these PEG and PEO samples.

Relations of the frequency shift and the bandwidth shift with the complex viscosity. Rearrangements of eqs (5) and (6) in the main text lead to the frequency shift

$$\Delta f_n = -\sqrt{\frac{n}{\pi\rho_q\mu_q}} f_0^{3/2} \sqrt{\rho_l \left(\sqrt{\eta'^2+\eta''^2} - \eta''\right)} \qquad \text{(S1)}$$

and the bandwidth shift

$$\Delta\Gamma_n = \sqrt{\frac{n}{\pi\rho_q\mu_q}} f_0^{3/2} \sqrt{\rho_l \left(\sqrt{\eta'^2+\eta''^2} + \eta''\right)} \qquad \text{(S2)}$$

On the other hand, the Voigt model relates the viscosity and elasticity of the overlay with the frequency shift and the dissipation shift via[1]

$$\Delta f_n = -\frac{1}{2\pi\rho_q h_q} \sqrt{\frac{\rho_l}{2}} \left[\eta\omega \sqrt{\frac{\sqrt{\mu^2+\eta^2\omega^2}+\mu}{\mu^2+\eta^2\omega^2}} - \mu \sqrt{\frac{\sqrt{\mu^2+\eta^2\omega^2}-\mu}{\mu^2+\eta^2\omega^2}} \right] \qquad \text{(S3)}$$

$$\Delta D_n = \frac{1}{\pi f_n \rho_q h_q} \sqrt{\frac{\rho_l}{2}} \left[\eta\omega \sqrt{\frac{\sqrt{\mu^2+\eta^2\omega^2}-\mu}{\mu^2+\eta^2\omega^2}} + \mu \sqrt{\frac{\sqrt{\mu^2+\eta^2\omega^2}+\mu}{\mu^2+\eta^2\omega^2}} \right] \qquad \text{(S4)}$$

where $h_q = (\mu_q/\rho_q)^{1/2}/2f_0$. After renaming the variables ($\mu \rightarrow \eta''\omega$, $\eta \rightarrow \eta'$),[2] the frequency shift can be written as

$$\Delta f_n = -\sqrt{\frac{n}{\pi\rho_q\mu_q}} f_0^{3/2}\sqrt{\rho_l}\left[\eta'\sqrt{\frac{\sqrt{\eta'^2+\eta''^2}+\eta''}{\eta'^2+\eta''^2}} - \eta''\sqrt{\frac{\sqrt{\eta'^2+\eta''^2}-\eta''}{\eta'^2+\eta''^2}}\right] \quad \text{(S5)}$$

and the bandwidth shif, $\Delta\Gamma_n = \Delta D_n f_n/2$, is

$$\Delta\Gamma_n = \sqrt{\frac{n}{\pi\rho_q\mu_q}} f_0^{3/2}\sqrt{\rho_l}\left[\eta'\sqrt{\frac{\sqrt{\eta'^2+\eta''^2}-\eta''}{\eta'^2+\eta''^2}} + \eta''\sqrt{\frac{\sqrt{\eta'^2+\eta''^2}+\eta''}{\eta'^2+\eta''^2}}\right] \quad \text{(S6)}$$

Apparently eqs (S1)-(S2) seem to take concise albeit different forms with eqs (S5)-(S6). In these equations, the pre-factor $K = \sqrt{\frac{n}{\pi\rho_q\mu_q}} f_0^{3/2}$ is a constant for each overtone. By assuming η' = $k\eta''$ with k the ratio between the dynamic viscosity and storage viscosity, these equations can be simplified to functions of η'' and k

$$\Delta f_n = -K\sqrt{\rho_l\eta''}\left[\sqrt{\sqrt{1+k^2}-1}\right] \quad \text{(S7)}$$

$$\Delta\Gamma_n = K\sqrt{\rho_l\eta''}\left[\sqrt{\sqrt{1+k^2}+1}\right] \quad \text{(S8)}$$

$$\Delta f_n = -K\sqrt{\rho_l\eta''}\left[k\sqrt{\frac{\sqrt{1+k^2}+1}{1+k^2}} - \sqrt{\frac{\sqrt{1+k^2}-1}{1+k^2}}\right] \quad \text{(S9)}$$

$$\Delta\Gamma_n = K\sqrt{\rho_l\eta''}\left[k\sqrt{\frac{\sqrt{1+k^2}-1}{1+k^2}} + \sqrt{\frac{\sqrt{1+k^2}+1}{1+k^2}}\right] \quad \text{(S10)}$$

We have plotted the terms in the square bracket as functions of k, and found those from eqs (S7)-(S8) coincide exactly with those from eqs (S9)-(S10). Actually some algebraic calculations show these equations are actually the same, since

$$\left[k\sqrt{\frac{\sqrt{1+k^2}+1}{1+k^2}} - \sqrt{\frac{\sqrt{1+k^2}-1}{1+k^2}}\right]^2 = \sqrt{1+k^2}-1 \quad \text{(S11)}$$

$$\left[k\sqrt{\frac{\sqrt{1+k^2}-1}{1+k^2}}+\sqrt{\frac{\sqrt{1+k^2}+1}{1+k^2}}\right]^2=\sqrt{1+k^2}+1 \qquad \text{(S12)}$$

Therefore we concluded that the procedures from eqs (5) and (6) and the Voigt model gave the same results.

Viscosity of sucrose solutions on the DOPC SLB. After forming supported lipid bilayer of DOPC on silicon oxide substrate, the adsorption behavior of sucrose solution was subsequently studied at sucrose weight fraction w_{sucrose} of 0.50, 1.0, 2.0, 5.0, 10.0, 20.0, 25.0, and 50.0%. The resonance frequency and the energy dissipation factor for all 7 harmonics (overtone number n = 1, 3, 5, 7, 9, 11, 13) were monitored as the sucrose solution pumping into the chamber followed by rinsing with water (Figure S1). The shifts in the resonance frequency and the energy dissipation factor induced by sucrose solution disappear as soon as the sucrose solutions had been rinsed away by water, indicating no irreversible adsorption. The plateau values of the frequency shift and the dissipation shift in the presence of sucrose solution were plotted as a function of the overtone number n, both showing the scaling laws of $-\Delta f_n/n \sim n^{-1/2}$ and $\Delta D_n \sim n^{-1/2}$ (Figure S2). The complex viscosities obtained from QCM-D show the behaviors of typical Newtonian fluids with dynamics viscosity η' = constant and storage viscosity η'' = 0, and the obtained η' agreed well with the bulk solution viscosity measured by a rheometer (Figure S3).

Scaling laws for the frequency shift, the dissipation factor shift, and the complex viscosities of PEG/PEO solutions on the normalized frequency. Figure S4 shows the dependence of the frequency shift-$\Delta f_n/n$, the dissipation factor shift ΔD_n on the normalized frequency $\omega\tau$. The scaling exponents decrease from -1/2 for low molecular weight PEG to -0.9 for high molecular weight PEG/PEO. Figure S5 shows the dependence of the polymer contributed complex viscosity on the normalized frequency in the region of $\omega\tau > 10$. The scaling

exponents for high molecular weight PEOs is about -0.41, in accord with the value of $1/(3\nu)-1$ with $\nu = 0.565$.

REFERENCES

1. Voinova, M. V.; Rodahl, M.;Jonson, M.; Kasemo, B. *Phys. Scripta* **1999**, *59*, 391-396.

2. Johannsmann, D. *The Quartz Crystal Microbalance in Soft Matter Research: Fundamentals and Modeling*; Springer, 2015.

Table S1. Molecular weight data of PEG and PEO samples.

sample[a]	supplier	M_w (g/mol)	M_n (g/mol)	M_w/M_n
PEG-200	SA[b]	201	183	1.10
PEG-400	SA	414	370	1.12
PEG-600	SA	631	591	1.07
PEG-1000	SA	992	936	1.06
PEG-1400	SA	1430	1350	1.06
PEG-2000	SA	2040	1980	1.03
PEG-4000	SA	4030	3900	1.03
PEG-6000	SA	5720	5430	1.05
PEG-8000	SA	8330	7970	1.05
PEG-10000	SA	10240	9450	1.08
PEG-20000	SA	19600	18160	1.08
PEG-35000	SA	31330	28650	1.09
PEO-116k	PL[c]	108700	99600	1.09
PEO-278k	PL	278700	248400	1.12
PEO-443k	PL	399900	312700	1.28

[a] The numbers in the sample name are weight-average molecular weight M_w as given by suppliers. [b] Sigma-Aldrich. [c] Polymer Laboratories Ltd.

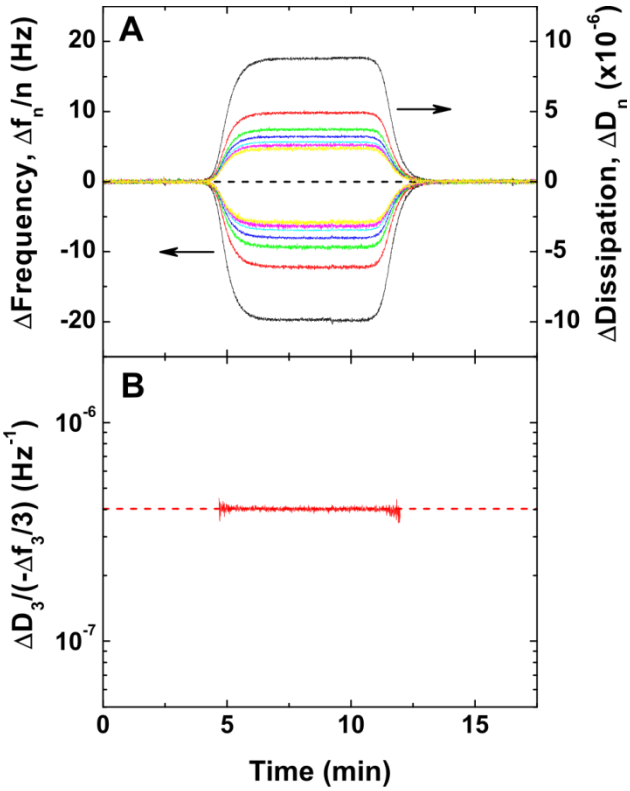

Figure S1. A typical QCM-D measurement for 2.0% sucrose aqueous solution on a SLB of DOPC. (A) The resonance frequency shifts $\Delta f_n/n$ and the energy dissipation shifts ΔD_n for all harmonics as a function of time. The frequency signals from bottom to top are for overtone number n = 1, 3, 5, 7, 9, 11, 13, respectively. The corresponding dissipation signals at each overtone are shown with the same color as frequency. (B) The ratio of dissipation shift to the frequency shift for the 3rd overtone, $\Delta D_3/(-\Delta f_3/3)$, as a function of time. A constant value very close to the theoretical value of $\Delta D_3/(-\Delta f_3/3) = 2/f_0$ (the red dashed line) was observed.

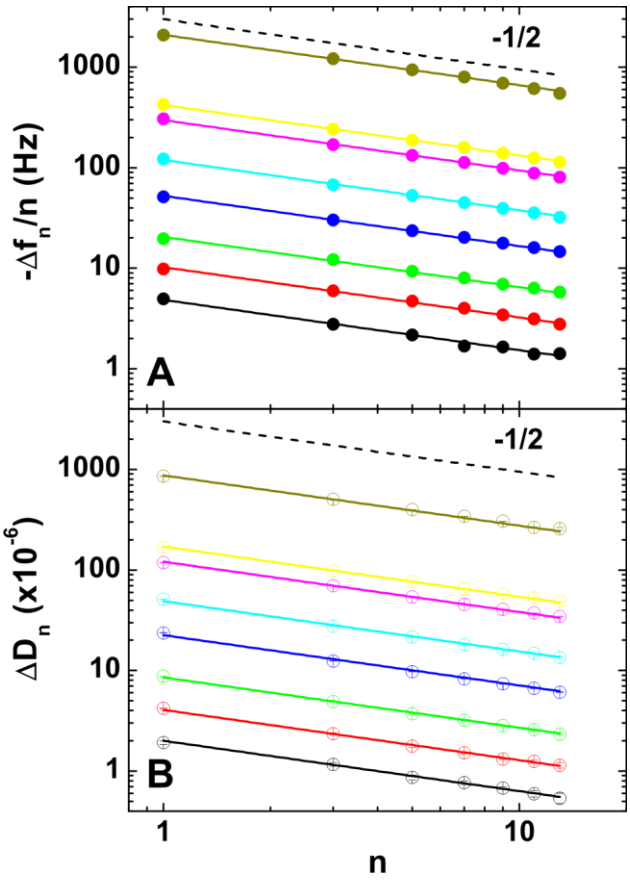

Figure S2. Dependence of (A) the frequency shifts $-\Delta f_n/n$ and (B) the dissipation shifts ΔD_n on the overtone number n. The data from bottom to top are for solution with sucrose weight fraction $w_{sucrose}$ of 0.50, 1.0, 2.0, 5.0, 10.0, 20.0, 25.0, and 50.0%, respectively. The solid lines are fitting to the data with scaling exponents of -1/2 (the dash lines serve as guides to the eyes).

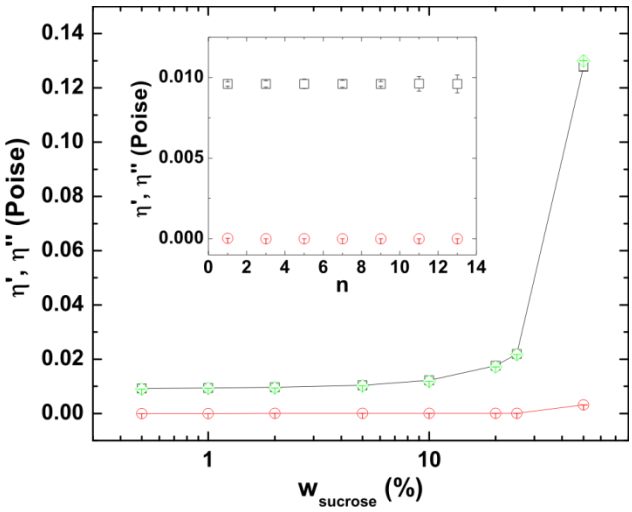

Figure S3. The dynamic viscosity η' (open squares) and storage viscosity η'' (open circles) of sucrose solution obtained from QCM-D as a function of sucrose weight fraction w_{sucrose}. The viscosity η of sucrose solution measured by a rheometer under steady shear flow is also shown (open diamond). The inset shows the complex viscosities of 2.0% sucrose solution for all harmonics from overtone number n = 1 up to 13.

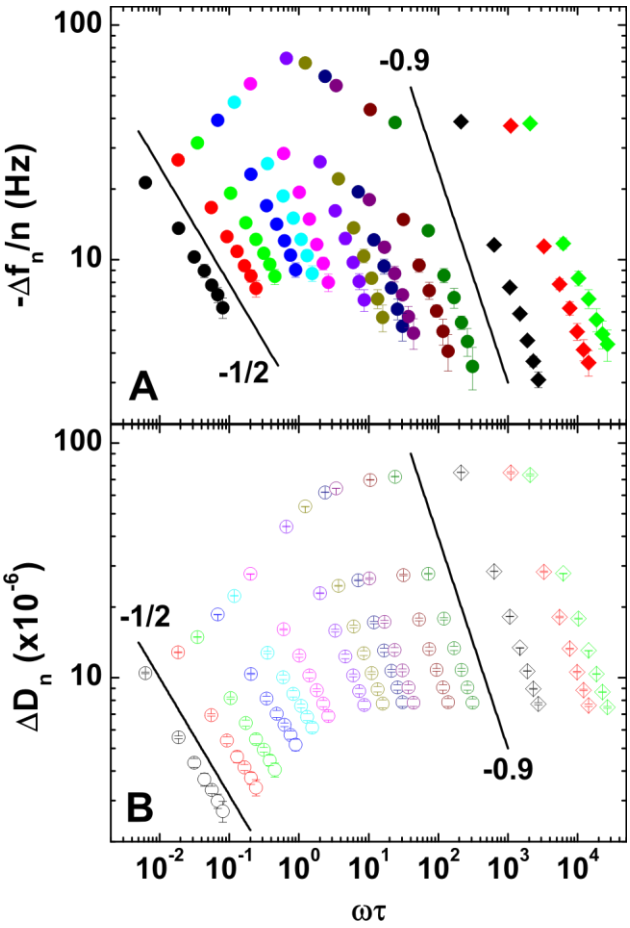

Figure S4. Dependence of (A) the frequency shifts $-\Delta f_n/n$ and (B) the dissipation shifts ΔD_n on $\omega\tau$ for 2.0% PEG/PEO aqueous solution on a SLB of DOPC. The data from left to right are for PEG/PEO with molecular weight of 200, 400, 600, 1000, 1400, 2000, 4000, 6000, 8000, 10000, 20000, 35000, 116k, 278k, and 443k, respectively. The solid lines serve as guides to the eye with scaling exponents of -1/2 for low molecular weight PEG and -0.9 for high molecular weight PEG/PEO.

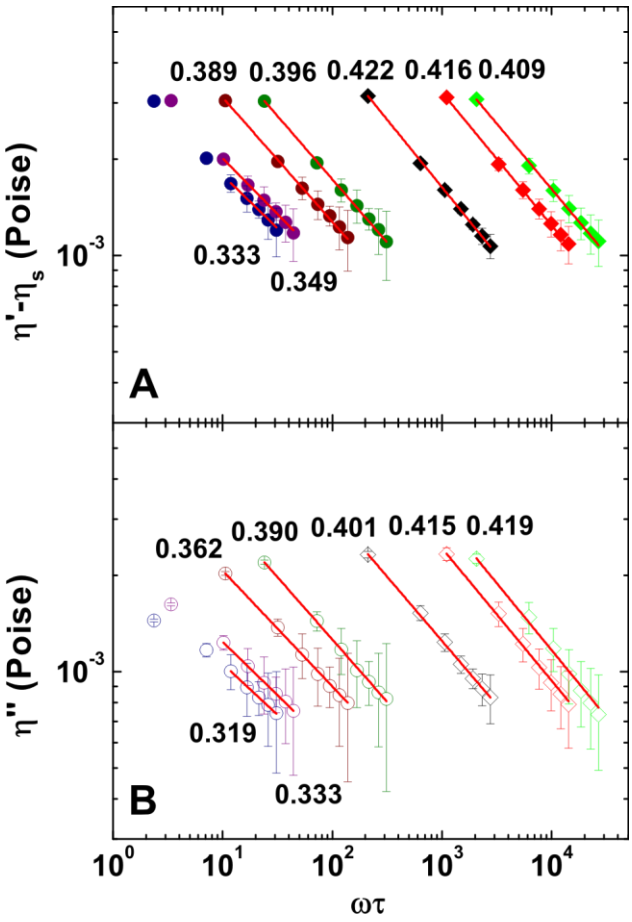

Figure S5. Dependence of polymer contributed dynamic viscosity η'-η_s (A) and storage viscosity η'' (B) on $\omega\tau$ for 2.0% PEG/PEO aqueous solution obtained from QCM-D. The data from left to right are for PEG/PEO with molecular weight of 8000, 10000, 20000, 35000, 116k, 278k, and 443k, respectively. The solid lines are fittings of the data in the region of $\omega\tau > 10$ to scaling laws and the obtained exponents are listed nearby.